# Land Use and Land Cover Change Analysis in Brazilian Urban centres: an approach using Cellular Automata and Neural Networks

Rodrigo José Zonzin Esteves[1,2], Andrés Velastegui-Montoya[3,4]
Mario Arthur Scalfani Pujatti[1,2], Leonardo José Silvestre[5], Marconi de Arruda Pereira[1]

[1] Departamento de Tecnologias (DTECH), Universidade Federal de São João del Rei (UFSJ), Ouro Branco, Brasil – rodrigojzonzin@aluno.ufsj.edu.br, mario_arthur_spujatti@aluno.ufsj.edu.br, marconi@ufsj.edu.br
[2] Departamento de Ciência da Computação (DCOMP), Universidade Federal de São João del Rei, São João del Rei, Brasil
[3] Centro de Investigación y Proyectos Aplicados a las Ciencias de la Tierra (CIPAT), ESPOL Polytechnic University, Guayaquil, Ecuador – dvelaste@espol.edu.ec
[4] Faculty of Engineering in Earth Sciences FICT, ESPOL Polytechnic University, Guayaquil, Ecuador
[5] Departamento de Computação e Eletrônica (DCE), Universidade Federal do Espírito Santo (UFES), São Mateus, Brasil – leonardo.silvestre@ufes.br

**Keywords:** Urban expansion, LULC, Remote sensing, CA-ANN model, Neural network

**Abstract**

During the 1970s, Brazil experienced most of its population living in cities for the first time. Historically, urbanization has been intensely related to land use and cover changes, amplifying climatic and ecological stress in recently established metropolises. This study aims to analyze, through classified Remote Sensing images and the Cellular Automata and Artificial Neural Networks (CA-ANN) machine learning model, land use and land cover trends in regions that have experienced accentuated demographic growth in the decades 2000 and 2010. The methodology consists of: i) identifying areas with a high density of buildings, ii) defining the variables that drive land use change, and iii) proposing a methodology for predicting changes in the urban area. The results indicate that the urban class prediction presented high precision (≥ 0.74) and recall (≥ 0.86) indices. Forest class also presented a high precision score (≥0.72), showing an elevated prediction hit rate. Furthermore, the proposed methodology improved the results obtained in previous works for the same cities, presenting higher Kappa values in all cases.

## 1. Introduction

Over the last century, the rapid intensification of urbanization has highlighted the growing scarcity of water, forests, and other natural resources, demonstrating that the expansion of urban areas is a critical factor in ecological imbalance (Zhang et al., 2022). The global urban population was 43% in 1990, increasing to 50% in 2007 and 56% in 2020 (Gu, Andreev and Dupre, 2021). By 2050, cities are expected to hold 68% of the world's population, causing more significant environmental pressure than the supply of available natural resources (UN, 2018). The main problem associated with the demographic increase is the need to expand urban infrastructure, such as the enlargement of the road network, greater capillarity of water and sewage supply, the requirement to modernize spaces and, above all, the demand for new areas of land occupation (Isamel, 2021; Stone, Hess and Frumkin, 2010).

In high-income countries, it is observed that urban expansion is well adapted to population growth, providing access to urban infrastructure such as housing, water and sewage treatment systems, and transportation (Wolch, Byrne and Newell, 2014). However, in developing countries, the growth of metropolises is not capable of meeting the demands of the progressive demographic increase, deepening spatial and socioeconomic inequalities and causing a heterogeneous scenario of soil changes at a global level (Sun et al., 2020 ).

In the Brazilian context, studies point to some determining components for urban expansion in the country's main metropolises (Camargo, Carmo and Anazawa, 2020; Freitas and Araki, 2021). It is known that, in addition to population growth, socioeconomic factors such as investment in urban infrastructure, travel time between home and work and increased per capita income contributed positively to urban expansion in metropolitan regions of Brazil (Silva, Esteves and Silva, 2024 ). In case studies on urban expansion patterns in Brazil, it was found that one of the main driving forces behind urban growth was the *Minha Casa Minha Vida* popular housing program, which intensified the dynamics of change in land use and land cover (LULC) at the same time it restructured urban infrastructure and contributed to migration of residents, commerce and services within city, (Correia Filho et al., 2022; Batista et al., 2021; Marques et al., 2021).

As a direct consequence of urban expansion, data from the Brazilian National Water and Sewage System (ANA) show that only 61.9% of the country's population is served by sewage collection, and 22.5% of this volume is discharged without treatment into nature (Borges et al., 2022). Another study shows that the rapid growth of cities has increased travel times in traffic, mainly due to the prevalence of individual transport in Brazil (Pereira et al., 2021).

In this context, it is verified that the dynamics of LULC involve a complex interrelationship of physical, geographic, economic and social variables. Several studies use earth observation data to assess the impacts of urban and population growth in the territory. For example, the Landsat satellite was used to assess global urban growth patterns between 1985 and 2015, and it was found that urban areas grew at a rate of 9,687 $km^2$/year (Liu et al., 2020). In Ethiopia, the prediction of urban expansion scenarios between 1968 and 2015 was modelled using Landsat satellite images, data on distance from the road network, digital elevation models and historical LULC images (Temesgen et al., 2021). Similarly, a study in Bangladesh uses Landsat images and surface temperature data to analyze the impact of urban growth on the generation of heat waves in city centres (Kafy et al., 2020). In both studies, the use of spatial variables such as distance from the road network, distance from rivers and maps of topographic aspects contributed significantly to the accuracy of the prediction models, highlighting a possible causal relationship between such aspects and the urban expansion phenomena.

Furthermore, studies evaluate LULC changes in the already urbanized regions of large Brazilian centres and forest frontier regions. In the State of Rondônia, in the Amazon, the use of classified Landsat images and spatial variables such as distance from highways and distance from urban centres was able to model and predict a deforestation rate of 27.50% in 2030 (Floreano and Moraes, 2021). Another work in southern Brazil analyzes which are the forces that direct the dynamics of LULC in the Chapecó Ecological Corridor, considering different scenarios of government action by using geographic, economic, technological and demographic variables to predict LULC change (Souza et al., 2023).

In this context, the objective of this work is to analyze trends in land use and land cover through the application of Remote Sensing classified data and the Cellular Automata - Artificial Neural Networks (CA-ANN) machine learning model to identify areas that are most susceptible to experiencing urban expansion. This work can be used to support local governments in proposing public policies to improve urban planning, ensuring the sustainable growth of the city and improving human development.

## 2. Materials and Methods

### 2.1 Study Area

According to IBGE data[1], ten Brazilian cities with the highest population growth between 2003 and 2013 were considered for this study. The ten cities in the study are located in 7 Brazilian states (Figure 1): Rio das Ostras, Macaé and Maricá in the state of Rio de Janeiro; Parauapebas and Barcarena in the state of Pará; Parnamirim in the state of Rio Grande do Norte; Rio Verde in Goiás; Palmas in Tocantins and Lauro de Freitas in Bahia.


Figure 1. Selected cities for analysis

The cities of Rio das Ostras, Maricá and Macaé are located in the Atlantic Forest biome on the coast of Rio de Janeiro State. These cities have average altitudes between 0 and 7 meters, and according to the Koppen classification, they have a tropical savanna climate, with a rainy season during December and March (Beck et al., 2018). On the other hand, the cities of Barcarena and Parauapebas, in Pará, are located in the Amazon, have a monsoon climate characterized by high temperatures, high precipitation, and low thermal amplitude and are part of the two main metropolitan centres in the State of Pará.

Moreover, the city of Parnamirim is located on the coast of the northeast region of Brazil, in the Atlantic Forest of Rio Grande do Norte State, with a tropical savanna climate and its relief characterized by the Brazilian Coastal Plain. Rio Verde, in Goiás, and Palmas, in Tocantins, are in the continent's interior. Both are inserted in the Brazilian Cerrado biome, which is characterized by extensive plateaus and presents a tropical savanna climate. In Maranhão, the city of São José de Ribamar is formed by mangrove vegetation, low altitude relief between 20 and 60 meters, and a tropical savanna climate.

### 2.2 Data Acquisition

Vector data of censitary municipal limits were obtained from the Brazilian Institute of Geography and Statistics (IBGE) website. These data were used as limits of the LULC rasters obtained from the MapBiomas project (MapBiomas, 2024). In addition, to include the influence of highways on urban growth, road network polygons were obtained for each city and made available by IBGE. Digital Elevation Models (DEMs) from the Shuttle Radar Topography Mission (SRTM) were also obtained on the Google Earth Engine (GEE) platform (NASA, 2000; Velastegui-Montoya et al., 2023).

### 2.3 Methodology

#### 2.3.1 Pre-processing

The censitary municipal polygons were inserted into GEE. Then, sectors considered to have a “High Density of Urban Building” were filtered to focus the processing on the main urban area of the municipality. Polygons with this characteristic consist of at least 250 residential buildings and 400 houses, forming adjacent sectors within a neighbourhood that exceed the maximum value (IBGE, 2024). After selecting the main urban area, a buffer of 100 meters was applied around the edges of the polygon to encompass transition aspects between urban and rural areas.

Following that, the polygons of the main urban areas were used to cut out the SRTM DEMs and IBGE highway data. In the next step, the MapBiomas rasters were reclassified into six classes encompassing the environment's main geophysical aspects (Table 1).

Then, a distance matrix was generated. It was necessary to convert the road network data into rasters to do this. After that, for each pixel of the Region of Interest (ROI) at position $P(x, y)$, the smallest distance that $P(x, y)$ expresses to any of the city's streets/roads is taken. This was possible by calculating the shortest Euclidean distance between each pixel of the urban area and a feature of the road network, obtaining a map of the proximity of the highways.

#### 2.3.2 Urban Expansion Analysis

The first step in analysing LULC changes is observing and selecting the variables composing the prediction model. This step was developed with the QGIS Modules for Land Use Change Evaluation (MOLUSCE) plugin. MOLUSCE is a tool that offers Artificial Neural Networks (ANN), Linear Regression and other geostatistical methods for LULC analysis and prediction

[1] https://agenciadenoticias.ibge.gov.br/agencia-sala-de-imprensa/2013-agencia-de-noticias/releases/13937-asi-censo-2010-populacao-do-brasil-e-de-190732694-pessoas. Access in 26/06/2024

(Aneesha Satya, Shashi and Deva, 2020). MOLUSCE has been used in other LULC prediction works, such as analysing LULC changes in Turkey (Değermenci, 2023) and modelling LULC and surface temperature in the city of Porto Alegre, Brazil (Fernandes et al., 2023).

The first step in modelling urban expansion was the insertion of LULC rasters at the initial and final dates of the period of interest. Furthermore, the spatial variables obtained included distance from the road network, the Mapbiomas raster time series for the period of interest, and the digital elevation models.

| Reclass. | Reclass. Value | MapBiomas Classification | MapBiomas Value |
|---|---|---|---|
| Forest | 1 | Forest Formation, Savanna Formation, Mangroove, Wooded Restinga | 1, 3, 4, 5, 49 |
| Non Forest | 2 | Non-Forest Natural Formation, Wetlands, Grassland, Salt flat, Rocky Outcrop, Other Non-Natural Formations | 10, 11, 12, 13, 29, 32 |
| Farming | 3 | Farming, Pasture, Agriculture, Tem. Crop, Soybean, Sugar Cane, Rice, Other Temp. Cros. Perennial Crop, Coffe, Citrus, Other | 14, 15, 18, 19, 39, 20, 40, 41, 36, 46, 47, 48, 9, 21 |
| Non Vegetated | 4 | Non-Vegetated Area, Beach, Dune, Sand Spot, Mining, Other Non-Veg. Areas | 22, 23, 30, 25 |
| Urban | 5 | Urban Area | 24 |
| Water | 6 | Water, River & Lake & Ocean, Agriculture | 26, 33, 31 |

Table 1. Thematic Reclassification of Mapbioma’s Data

Pearson's correlation coefficient was calculated to verify linearity in the relationship between classes. The normalised dot product between the variables under analysis gives the Pearson correlation coefficient, assuming values between -1 and 1 for high negative and positive correlations, respectively (Deisenroth, Faisal and Ong, 2020).

After checking the linearity between the data, the next step involves generating a class transition matrix. The analysis of changes in LULC categories over time represents the portions of pixels susceptible to class switching. In this matrix, values close to 1 represent the stability of the class (the proportion between current use/previous use). In contrast, values close to zero represent variation in class use.

After creating the transition and correlation matrices, a transition map is generated to evaluate the change between each combination of classes under analysis. This map is twice the size of the original classes, as changes must be evaluated for each element in the Cartesian product ImginitImgfinal. For example, in an analysis involving two classes – forest and city – changes between forest-forest, forest-city, city-forest, and city-city must be evaluated.

After generating the maps, the machine learning model that will predict LULC changes was defined. The Cellular Automata and Artificial Neural Networks (CA-ANN) model is a tool used in various types of studies for the future simulation of LULC (Guan et al., 2011; Wang, Munkhnasan and Lee 2021). This approach has been used to predict spatial changes due to the ability to estimate the current condition of each pixel based on the initial conditions, adjacency and direction laws of LULC changes captured by the transition matrix. Furthermore, this method can accurately analyse non-linear spatial relations in the LULC change process, also considering stochastic processes for changing land use and occupation.

The neural network in the CA-ANN model requires five initialisation hyperparameters. The first hyperparameter to be calibrated is Neighborhood, which determines the number of pixels evaluated around a given point under analysis. For example, for the value 1, 9 *(3x3)* pixels will be evaluated, 1 pixel in each grid direction. For the value of 2 pixels, 25 *(5x5)* pixels will be evaluated, and so on.

Another hyperparameter is the Learning Rate, an adjustment coefficient to scale the update of the network's weights during the execution of the Back Propagation algorithm. Updating the weight vector of a neural network involves the products of the adjustment coefficient, error and current weights. Hence, the Learning Rate scales the update rate of the Network parameters, impacting the speed and quality of the network's learning.

Furthermore, optimising the hyperparameters encompassed the values of Momentum and Maximum Iterations, representing a heuristic for the Stochastic Gradient Descent algorithm and a stopping condition, respectively. The values were defined following the previous study: Neighbourhood: 5 px, Learning rate: 0.100, Maximum Iterations: 1000, Momentum: 0.050 and Hidden Layers: 10 (Pujatti, de Arruda and Silvestre, 2022).

After defining the hyperparameters, the training of the network for each city under analysis was conducted. At the end of each training, a LULC map was generated for the analysed period. Finally, LULC images from MapBiomas were used to validate the results, obtain the Kappa index metrics, and measure the model's reliability.

Then, using Python, the validation LULC and the predicted LULC were used to construct the confusion matrix. In this way, the sensitivity, accuracy, recall and F1-score metrics were obtained to evaluate the model's performance.

## 3. Results

To evaluate the result of the predictions, Figure 2 presents the LULC images of the 10 Brazilian cities in 2020 and the corresponding prediction obtained by MOLUSCE for the same year. Table 2 presents the accuracy obtained by the model for each city under analysis. Similarly, Table 3 presents the recall results.

The lowest accuracy was identified in the city of Parnamirim (0.89). In the centre of the city's study region, the non-vegetated class (class 4) presented the most significant error. This occurs because this extensive region is located at the Natal Air Base, which has pixels of urban infrastructure and bare soil. The variability of the spectral response of the pixels over the years

contributed to an irregular LULC classification, so the model could not identify a pattern of LULC change. In the forestry class, which also showed a deviation in relation to actual occupation, a sparseness of pixels was observed along the southern part of the city, where there is an intense presence of high-end housing developments.

The conversion of a pixel in the region led the model to infer that the surrounding areas would also be modified, while the conservation of the forest region was actually observed.

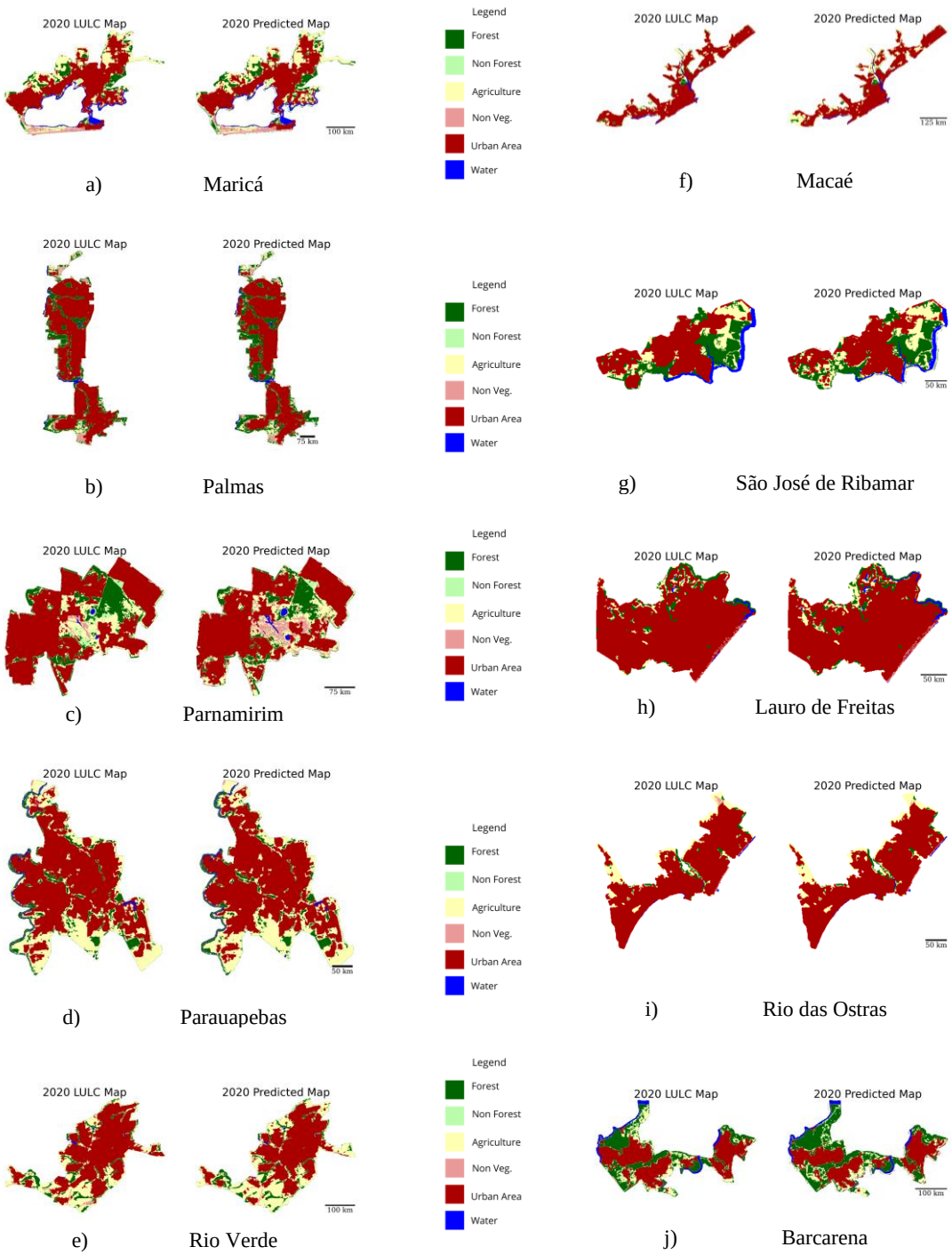


Figure 2: Comparison between Predicted LULC and 2020 MapBiomas LULC

The São José de Ribamar and Parauapebas cities presented a higher rate of satisfactory predictions (0.92). When predicting the areas of São José de Ribamar, the model overestimated the urban occupation in the southwest portion of the city, where there is a less significant occupation of urbanized settlements, and underestimated the area transition from pasture to city, to the northeast of the main urban area. The precision of the non-forested class was the most sensitive to error, presenting

Precision = 0.29. However, in Parauapebas, the main limitation was observed in predicting non-vegetated areas, especially in the Jardim Tropical neighbourhood in the extreme north of the city. Conversely, the prediction of forest areas proved consistent, showing slight variation along the Parauapebas River, where there is a Permanent Preservation Area (BRASIL, 2012) and an Accuracy of 0.81. Some areas of vegetation within the main urban area were suppressed or decreased in the prediction..

In the cities of the State of Rio de Janeiro, high accuracy rates were obtained in Marica (0.97) and Macaé (0.98). The main feature observed for the city of Maricá was the urban occupation southeast of the region of interest, which the model underestimated. For Macaé, the class of agricultural features was the most sensitive to errors, presenting the lowest F1-Score in the prediction (0.67). For this class, pixels from agricultural areas were well classified (Recall = 0.86), although, of all pixels labelled as this class, a portion of 0.54 was agricultural pixels (Precision = 0.54).

In the Cerrado Biome, Palmas (Accuracy = 0.95) and Rio Verde (Accuracy = 0.95) showed a similar behaviour. In the same way that Palmas successfully identified the principal axes of forest preservation (Precision = 0.72), Rio Verde also successfully defined them (Precision = 0.86), presenting lower precision for the non-vegetated class (0.29). Of all urban areas in Rio Verde and Palmas, the model correctly detected a fraction of Recall = 0.86 and Recall = 0.84, respectively.

The analysis of the city of Barcarena demonstrates an accuracy rate of 0.97 for the urban class, whose main limitation was observed in the region of the Itupanema Neighborhood, close to the Amazon Logistics Terminal, inaugurated in 2023 (Cintra, 2023). Furthermore, considering all pixels predicted as urban, the verified correctness rate (Recall) was 0.85, indicating a high hit rate for the model. The Precision and Recall values for the Non-Vegetable class were zero since no pixels of this class were observed in the city. The forest class presented 0.92 Recall, indicating that the model successfully identified the areas that were actually forested.

For the city of Lauro de Freitas, the accuracy rate for the urban class was 1.00. This result is explained by the fact that the model did not present any false-positive pixels; that is, all pixels predicted for the urban class were, in fact, from the urban class. On the other hand, the model generalized urban occupation beyond truth-ground observed data: a rate of 0.96 of the pixels considered urban were, in fact, urban. When looking at the city's 2020 LULC map, it is clear that the urban class occupation density contributed to the high Precision and Recall rate. Furthermore, the analysis of the non-forest class showed a Precision value of 0.03, and of all predictions in this class, 0.10 were correct (Recall). For forestry, agriculture and water bodies classes, F1-score rates of 0.74, 0.54 and 0.64, respectively, were obtained.

The present work presented notable results in relation to works that developed similar methodologies. For Barcarena, Lauro de Freitas and Parauapebas, the proposed methodology obtained Kappa indices of 0.87604, 0.93183 and 0.86810, respectively. The present methodology provides complementary evidence to the Kappa index analysis 0.83193, 0.78486 and 0.81884 for the respective cities (Pujatti et al., 2022).

| | Forest | Non Forest | Farm. | Non Veg | Urban Area | Water |
|---|---|---|---|---|---|---|
| Barcarena | 0.73 | 0.44 | 0.57 | 0.00 | 0.97 | 0.97 |
| Lauro de Freitas | 0.72 | 0.03 | 0.47 | 0.60 | 1.00 | 0.49 |
| Macaé | 0.74 | 0.82 | 0.54 | 0.70 | 0.97 | 0.89 |
| Maricá | 0.72 | 0.91 | 0.81 | 0.89 | 1.00 | 0.98 |
| Palmas | 0.72 | 0.43 | 0.52 | 0.61 | 1.00 | 0.84 |
| Parnamirim | 0.82 | 0.38 | 0.48 | 0.12 | 0.99 | 0.39 |
| Rio Verde | 0.81 | 0.77 | 0.69 | 0.29 | 1.00 | 0.86 |
| São José de Ribamar | 0.81 | 0.29 | 0.62 | 0.81 | 0.99 | 0.92 |
| Parauapebas | 0.81 | 0.82 | 0.98 | 0.42 | 0.74 | 0.88 |
| Rio das Ostras | 0.73 | 0.85 | 0.98 | 0.43 | 0.96 | 0.88 |

Table 2. Precision

| | Forest | Non Forest | Farm. | Non Veg | Urban Area | Water |
|---|---|---|---|---|---|---|
| Barcarena | 0.92 | 0.74 | 0.5 | 0.00 | 0.85 | 0.97 |
| Lauro de Freitas | 0.77 | 0.10 | 0.64 | 0.90 | 0.96 | 0.92 |
| Macaé | 0.66 | 0.79 | 0.86 | 0.75 | 0.89 | 0.89 |
| Maricá | 0.90 | 0.89 | 0.89 | 0.93 | 0.93 | 0.95 |
| Palmas | 0.81 | 0.55 | 0.57 | 0.56 | 0.95 | 0.90 |
| Parnamirim | 0.74 | 0.31 | 0.53 | 0.66 | 0.91 | 0.99 |
| Rio Verde | 0.88 | 0.77 | 0.93 | 0.21 | 0.86 | 0.78 |
| São José de Ribamar | 0.99 | 0.86 | 0.56 | 0.80 | 0.90 | 0.80 |
| Parauapebas | 0.89 | 0.64 | 0.65 | 0.96 | 1.00 | 0.96 |
| Rio das Ostras | 0.93 | 0.84 | 0.76 | 0.46 | 0.96 | 0.69 |

Table 3: Recall

## 4. Conclusions

Earth Observation studies have been a well-established source of information for public policies aimed at social progress and defence. Similarly, while using Artificial Intelligence has raised questions about its impacts on human relationships, its application in scientific methods has notably provided high-quality results. This study uses the CA-ANN model to filter Remote Sensing images of densely populated urban building areas, aiming to model the expansion trends of major urban centres in the fastest-growing cities of Brazil.

In this sense, the results allowed a consistent analysis of land use and cover patterns in the cities under study. The prediction of urban classes and water bodies presented high precision and recall rates, allowing a significant prediction of LULC trends in urban planning. Furthermore, the water body class prediction also showed high precision and recall rates, explained by the spatio-temporal immutability in most scenes. Despite this, the prediction of classes that present photosynthetic activity can guarantee valuable information for managing critical areas around water bodies, as is the case in Parauapebas. Moreover, the results revealed considerable variations in the accuracy of predictions, influenced by the particularities of each city. An example is the city of Parnamirim, which contains the Natal Air Base in the study region, shifting the results of non-urban classes to lower results..

Finally, future work can deepen the quality of the results obtained by comparing the prediction of urban areas when there is a focus on the main urban area using other LULC prediction models. Furthermore, including economic, social, population, cultural variables, and others can contribute to a more accurate model for predicting the spread of the urban area..

## References

Aneesha Satya, B., Shashi, M., Deva, P., 2020. Future land use land cover scenario simulation using open source GIS for the city of Warangal, Telangana, India. *Applied Geomatics*, 12(3). https://doi.org/10.1007/s12518-020-00298-4

Batista, B. A., Correia Filho, W. L. F., Oliveira-Júnior, J. F. de, Santiago, D. de B.,, Santos, C. T. dos., 2021. Avaliação da expansão urbana na Cidade de Maceió, Alagoas – Nordeste do Brasil. *Research, Society and Development*, 10(11). https://doi.org/10.33448/rsd-v10i11.19537

Beck, H. E., Zimmermann, N. E., McVicar, T. R., Vergopolan, N., Berg, A., Wood, E. F., 2018. Present and future köppen-geiger climate classification maps at 1-km resolution. *Scientific Data*, 5. https://doi.org/10.1038/sdata.2018.214

Borges, M. C. P., Abreu, S. B., Lima, C. H. R., Cardoso, T., Yonamine, S. M., Araujo, W. D. V., Silva, P. R. S., Machado, V. B., Moraes, V., Silva, T. J. B., Reis, V. A., Santos, J. V. R., Reis, M. L., Canamary, É. A., Vieira, G. C., Meireles, S., 2022. The Brazilian National System for Water and Sanitation Data (SNIS): Providing information on a municipal level on water and sanitation services. *Journal of Urban Management*, 11(4). https://doi.org/10.1016/j.jum.2022.08.002

BRASIL. Lei nº 12.651, de 25 de maio de 2012. Institui o novo código florestal brasileiro.

Camargo, K. C. de M., Carmo, R. L. do, Anazawa, T. M., 2020. Breves considerações sobre expansão urbana nas megacidades da América Latina: o caso de São Paulo. *Revista Espinhaço*, 9(2). https://doi.org/10.5281/zenodo.443445

Cintra, A. L., 2023, nov. 28th. Grupo empresarial inaugura terminal logístico estratégico no Pará. *Belém Negócios*. https://www.belemnegocios.com/post/grupo-empresarial-inaugura-terminal-logistico-estrategico-no-para

Correia Filho, W. L. F., Oliveira-Júnior, J. F. de, Santos, C. T. B. dos, Batista, B. A., Santiago, D. de B., Silva Junior, C. A. da, Teodoro, P. E., Costa, C. E. S. da, Silva, E. B. da, Freire, F. M., 2022. The influence of urban expansion in the socio-economic, demographic, and environmental indicators in the City of Arapiraca-Alagoas, Brazil. *Remote Sensing Applications: Society and Environment*, 25. https://doi.org/10.1016/j.rsase.2021.100662

Değermenci, A. S., 2023. Spatio-temporal change analysis and prediction of land use and land cover changes using CA-ANN model. *Environmental Monitoring and Assessment*, 195(10). https://doi.org/10.1007/s10661-023-11848-9

Deisenroth, M. P., Faisal, A. A, Ong, C. S., 2020. Mathematics for Machine Learning. *Cambridge University Press.*

Fernandes, R. P., 2023. Zonas climáticas e ilhas de calor urbanas da superfície em Porto Alegre (RS - Brasil) entre 2002 e 2023 (Mestrado em Sensoriamento Remoto e Geoprocessamento). *Universidade Federal do Rio Grande do Sul.* http://hdl.handle.net/10183/271901

Floreano, I. X., de Moraes, L. A. F, 2021. Land use/land cover (LULC) analysis (2009–2019) with Google Earth Engine and 2030 prediction using Markov-CA in the Rondônia State, Brazil. *Environmental Monitoring and Assessment*, 193(4). https://doi.org/10.1007/s10661-021-09016-y

Freitas, E. V., Araki, H., 2021. Simulation of urban growth: A case study for Curitiba city, Brazil. *Boletim de Ciencias Geodesicas*, 27(Special issue). https://doi.org/10.1590/s1982-21702021000s00019

Guan, D. J., Li, H. F., Inohae, T., Su, W., Nagaie, T., Hokao, K., 2011. Modelling urban land use change by the integration of cellular automata and Markov model. *Ecological Modelling*, 222(20–22). https://doi.org/10.1016/j.ecolmodel.2011.09.009

IBGE, 2024. Instituto Brasileiro de Geografia e Estatística (IBGE). *Malha de Setores Censitários preliminares*. Retrieved from: https://biblioteca.ibge.gov.br/visualizacao/livros/liv102072.pdf

Ismael, H. M., 2021. Urban form study: the sprawling city—review of methods of studying urban sprawl. *GeoJournal*, *86*(4). https://doi.org/10.1007/s10708-020-10157-9

Kafy, A. al, Rahman, M. S., Faisal, A. al, Hasan, M. M., Islam, M, 2020. Modelling future land use land cover changes and their impacts on land surface temperatures in Rajshahi, Bangladesh. *Remote Sensing Applications: Society and Environment*, 18. https://doi.org/10.1016/j.rsase.2020.100314

Liu, X., Huang, Y., Xu, X., Li, X., Li, X., Ciais, P., Lin, P., Gong, K., Ziegler, A. D., Chen, A., Gong, P., Chen, J., Hu, G., Chen, Y., Wang, S., Wu, Q., Huang, K., Estes, L., Zeng, Z., 2020. High-spatiotemporal-resolution mapping of global urban change from 1985 to 2015. *Nature Sustainability*, 3(7). https://doi.org/10.1038/s41893-020-0521-x

MapBiomas. Coleção 8 da Série Anual de Mapas de Cobertura e Uso da Terra do Brasil. https://brasil.mapbiomas.org/

Marques, M. L., Müller-Pessôa, V., Camargo, D., Cecagno, C., 2021: Simulação de cenários urbanos por autômato celular para modelagem do crescimento de Campinas - sp, Brasil. *Eure*, 47(142). https://doi.org/10.7764/eure.47.142.10

NASA, 2000. National Aeronautics and Space Administration (NASA). *Shuttle Radar Topography Mission (SRTM).* Retrieved from: https://www.earthdata.nasa.gov/sensors/srtm

Pujatti, M. A. S., de Arruda Pereira, M., Silvestre, L. J., 2022. A tool to predict the growth of urban regions based on QGIS/MOLUSCE using MapBiomas image time series. *Proceedings of the Brazilian Symposium on GeoInformatics.*

Silva, R. R., Esteves, R. J. Z., Silva, K. A. F., 2024: A expansão Urbana Das Principais metrópoles Brasileiras De 2000 a 2020. *Cuadernos De Educación Y Desarrollo 16 (4):* e4074. https://doi.org/10.55905/cuadv16n4-159

Souza, J. M. de, Morgado, P., Costa, E. M. da, Vianna, L. F. de N., 2023. Predictive Scenarios of LULC Changes Supporting Public Policies: The Case of Chapecó River Ecological Corridor, Santa Catarina/Brazil. *Land*, 12(1). https://doi.org/10.3390/land12010181

Stone, B., Hess, J. J., Frumkin, H., 2010. Urban form and extreme heat events: Are sprawling cities more vulnerable to climate change than compact cities? *Environmental Health Perspectives*, 118(10). https://doi.org/10.1289/ehp.0901879

Sun, L., Chen, J., Li, Q., Huang, D., 2020. Dramatic uneven urbanization of large cities throughout the world in recent decades. *Nature Communications*, 11(1). https://doi.org/10.1038/s41467-020-19158-1

Temesgen, H., Wu, W., Legesse, A., Yirsaw, E., 2021. Modelling and prediction of effects of land use change in an agroforestry dominated southeastern Rift-Valley escarpment of Ethiopia. *Remote Sensing Applications: Society and Environment*, 21. https://doi.org/10.1016/j.rsase.2021.100469

UN, 2019. Department of Economic and Social Affairs, Population Division (2019). World Population Prospects 2018: Highlights (ST/ESA/SER.A/421). *In Department of Economic and Social Affairs, Population Division (2019). World Population Prospects 2018: Highlights* (ST/ESA/SER.A/421).

Wang, S. W., Munkhnasan, L., & Lee, W. K., 2021: Land use and land cover change detection and prediction in Bhutan’s high altitude city of Thimphu, using cellular automata and Markov chain. *Environmental Challenges*, 2. https://doi.org/10.1016/j.envc.2020.100017

Velastegui-Montoya, A., Montalván-Burbano, N., Carrión-Mero, P., Rivera-Torres, H., Sadeck, L. Adami, M., 2023. Google Earth Engine: A Global Analysis and Future Trends. *Remote Sensing*, 15(14). https://doi.org/10.3390/rs15143675

Wolch, J. R., Byrne, J., Newell, J. P., 2014. Urban green space, public health, and environmental justice: The challenge of making cities “just green enough.”. *Landscape and Urban Planning*, 125. https://doi.org/10.1016/j.landurbplan.2014.01.017

Zhang, M., Du, H., Zhou, G., Mao, F., Li, X., Zhou, L., Zhu, D., Xu, Y., Huang, Z., 2022. Spatiotemporal Patterns and Driving Force of Urbanization and Its Impact on Urban Ecology. *Remote Sensing*, 14(5). https://doi.org/10.3390/rs14051160